AIChE WILEY InterScience DISCOVER SOMETHING GREAT

Proteins Separation and Purification by Salt Gradient Ion-Exchange SMB

Ping Li, Guohua Xiu, and Alirio E. Rodrigues
Laboratory of Separation and Reaction Engineering, Dept. of Chemical Engineering, Faculty of Engineering, University of Porto, Rua Dr. Roberto Frias, s/n 4200-465 Porto, Portugal

DOI 10.1002/aic.11259
Published online August 1, 2007 in Wiley InterScience (www.interscience.wiley.com).

The process performance of the separation and purification of proteins by ion-exchange simulated moving bed (IE-SMB) can be improved when a step-wise salt concentration is formed in the SMB unit, called salt gradient IE-SMB. In this paper, a gradient SMB model is used to analyze the performance of the salt gradient IE-SMB process, based on literature data for linear adsorption of proteins. Some strategies are discussed for the selection of salt gradient in IE-SMB chromatography for proteins effective separation. Three configurations of the gradient SMB process, open loop, closed loop, and closed loop with a holding vessel are compared. When running a gradient SMB with closed loop configuration, a holding vessel with a given volume is added to the system to mix online the desorbent with the recycled stream from section IV during the switching interval, in order to reduce the fluctuation of salt or solvent strength in the columns. Moreover, we also present a comparison of two strategies of modeling, the gradient SMB model and the equivalent gradient TMB model, for the prediction of internal concentration profiles in gradient SMB chromatography with open loop and closed loop, respectively. © 2007 American Institute of Chemical Engineers *AIChE J,* 53: 2419–2431, 2007

Keywords: simulated moving bed (SMB), gradient simulated moving bed, salt gradient, ion-exchange, proteins separation, protein purification, protein adsorption, modeling

Introduction

Simulated moving bed (SMB) chromatography is a continuous process, which for preparative purposes can replace the discontinuous elution chromatography. Furthermore, the countercurrent contact between fluid and solid phase used in SMB chromatography maximizes the mass transfer driving force, leading to a significant reduction of mobile phase consumption and solid phase requirements when compared with elution chromatography. With the developed theory and technique,[1–5] the resolution of similar products on preparative scale (ktons/year) can be performed efficiently using SMB chromatography. Successful examples are the separation of *p*-xylene from a mixture of C8 isomers, the separation of glucose and fructose, and the resolution of enantiomers on chiral stationary phases.[1,2,6–8] The new challenge for the SMB technology is its application to the separation and purification of biomolecules; examples of products that are considered for SMB separation and purification are therapeutical proteins, antibodies, nucleosides, and plasmid DNA.[9–17]

Research on the separation and purification of proteins by SMB technology started with size-exclusion SMB (SE-SMB) chromatography, for its design simplicity in terms of the liquid and solid flow rate ratios (linear distribution coefficients for all proteins on porous stationary phases). Experimental examples are: insulin purification by SE-SMB packed with

Correspondence concerning this article should be addressed to A. E. Rodrigues at arodrig@fe.up.pt.
Current address of P. Li: College of Resource and Environmental Engineering, East China University of Science and Technology, Shanghai 200237, China.
Current address of G. Xiu: BOC Technology center (China), JinZang Rd. 258, Pudong, Shanghai 201206, China.

Sephadex G50 gel,[12] purification of plasmid DNA by SE-SMB packed with Sepharose FF particles,[13,16] and separation of bovine serum albumin (BSA) and myoglobin by SE-SMB packed with Sepharose Big Beads.[17] Because of the absence of ligand in these particles, the distribution coefficients of proteins depend only on the accessible porosity in the particles. A large protein has a smaller distribution coefficient, as weakly retained component, and will elute in the raffinate stream; in contrast, a small protein has a bigger distribution coefficient, as strongly retained component, will elute from the extract stream in the SE-SMB. It is easy to obtain a large protein molecule with high purity from the raffinate stream, but it is difficult to recover the smaller protein molecule with high purity protein in the extract stream because of the limitation of the mass transfer resistance of the larger protein molecule.[17]

As a result of the limitation of SE-SMB technology for the separation and purification of proteins, research was extended to the application of ion-exchange SMB (IE-SMB), reversed-phase SMB (RP-SMB), and affinity SMB (A-SMB).[11,18,19] By carefully selecting the buffer, pH value, solvent strength, and ligand of adsorbent to ensure that the larger protein molecule elutes from the extract stream, while the smaller protein is recovered from the raffinate stream, the two proteins can be separated efficiently by the SMB technology. When the binding capacities of proteins on the adsorbent are close to each other, an isocratic SMB mode may be used to separate the proteins, where the adsorbents have the same binding capacity to protein in all sections of the SMB unit, as shown in Figure 1a. However, the binding capacities of proteins on adsorbents are usually so different in ion-exchange, hydrophobic-interaction, reversed-phase, and affinity chromatography (IEC, HIC, RPC, and AC) that we cannot separate them in the isocratic mode with a reasonable retention time. In the conventional elution chromatography, a gradient mode should be used for the separation of proteins; for example, organic solvent gradient in RPC, and salt gradient in IEC, either in step-wise gradient or linear gradient. In the SMB unit, a step-wise gradient can be formed easily by introducing a solvent mixture with a lower strength at the feed inlet port compared to the solvent mixture introduced at the desorbent port; then the adsorbent has a lower binding capacity for protein in section I and II to improve the desorption, and a stronger binding capacity in section III and IV to increase the adsorption, as shown in Figure 1b. Some authors[11,18,20–24] stated that the solvent consumption by the gradient mode can be decreased significantly when compared with the isocratic SMB chromatography. Moreover, when a given feed is applied to the gradient SMB chromatography, the protein obtained from the extract stream can be enriched if the protein has a medium or high solubility in the solution with the stronger solvent strength, while the raffinate protein is not diluted at all.[18]

Experimental research for the separation of proteins by salt gradient IE-SMB[11] and for the separation of antibodies by solvent gradient RP-SMB[25] allowed a qualitative analysis of process feasibility. Furthermore, theoretical analysis for gradient SMB reported by some authors[11,18,20–24] confirmed the potential application of the gradient SMB technology in bioseparation. Up to now, this research is just underway partly because experiments are expensive (expensive proteins, special adsorbent, and SMB unit) for the practical separation and purification of proteins by the gradient SMB chromatography. Therefore, a detailed mathematical simulation, using a gradient SMB model instead of an equivalent gradient TMB model, is more significant to understand the performance of the gradient SMB chromatography. One objective of this paper is to simulate the salt gradient IE-SMB processes by using the gradient SMB model.

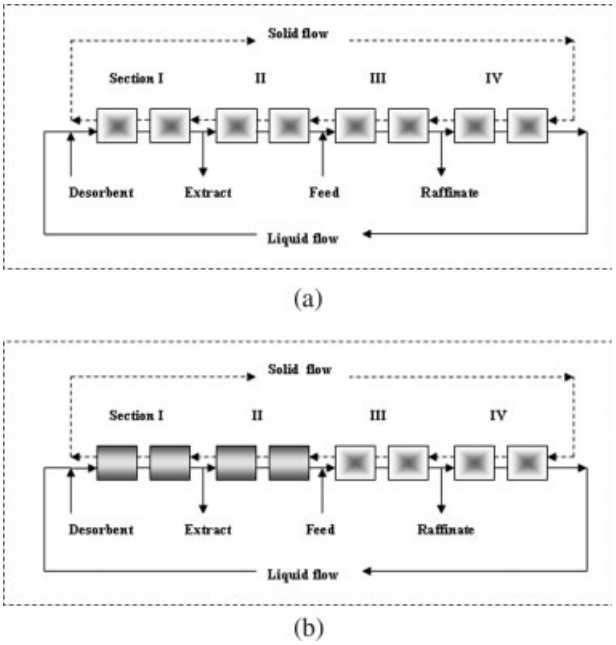

Figure 1. Schematic diagram of a four-zone isocratic/gradient SMB with closed loop.

(a) Isocratic SMB with closed loop; (b) gradient SMB with closed loop. ( ): higher solvent strength; ( ): lower solvent strength.

The open loop configuration was used by many authors to avoid the accumulation of contaminants in the columns of SMB for the separation and purification of proteins, as shown in Figure 2a, where the liquid stream from section IV is discarded, instead of being recycled to the desorbent stream allowing the reduction of desorbent consumption. It is well known that one of the biggest advantages of SMB chromatography compared with fixed bed chromatography is the lower desorbent consumption. This can be achieved in the closed loop configuration by recycling the liquid stream from section IV to the desorbent inlet of section I, as shown in Figure 2b, which is also important for RP-SMB because of the large amount of organic solvent being consumed. However, the recycle of liquid stream is more complicated for the gradient SMB chromatography. The solvent strength in the eluent is different between sections I and IV, and the composition of the stream leaving section IV varies in a dynamic manner during the switching interval, which complicates the direct recycling of the eluent.[25] In Figure 2c, a holding vessel with a given volume is added to the system to mix online the desorbent with the recycled liquid stream from section IV during the switching interval, to reduce the fluctuation of

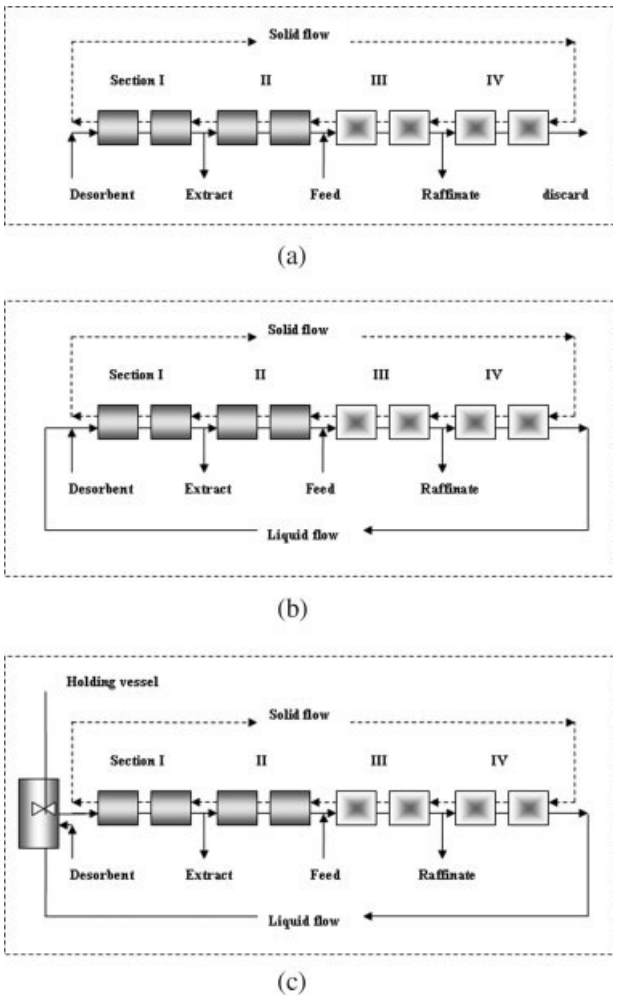

Figure 2. Operation modes for gradient SMB.

(a) Gradient SMB with open loop; (b) gradient SMB with closed loop; (c) gradient SMB with closed loop and a holding vessel. (■): higher solvent strength; (■): lower solvent strength.

the solvent strength in the columns. Another objective of this paper is to evaluate and compare three different configurations of gradient SMB: open loop (Figure 2a), closed loop (Figure 2b), and closed loop with a holding vessel (Figure 2c).

Gradient SMB Strategies of Modeling

Formation of salt gradient in the IE-SMB chromatography

A four-zone SMB chromatography is shown in Figure 1, and is constituted by a set of identical fixed-bed columns, which are connected in series. Each column is packed with Q-Sepharose FF resin. Q-Sepharose FF resin is a strong anion exchanger with $-CH_2-N^+-(CH_3)_3$ functional group; its matrix consists of macroporous crosslinked 6% agarose gel with a particle density of 1050 kg/m^3 (drained particle, measured by pycnometry) and a mean particle size of 90 μm (a particle size distribution of 45–165 μm). Q-Sepharose FF resin was purchased from Amersham Pharmacia Biotech. It is well known that the binding capacity of the classical ion exchanger to proteins is sensitive to salt concentration in the feedstock; the higher the salt concentration is, the lower the binding capacity to the proteins is. Therefore, a step-wise gradient is formed by introducing a lower salt concentration at the feed port compared to a higher salt concentration introduced at the desorbent port; then the ion exchanger has a lower binding capacity for proteins in sections I and II to improve the desorption and has a stronger binding capacity in sections III and IV to increase adsorption in the IE-SMB chromatography.

Model equations for the gradient SMB model

Model equations for the gradient SMB model result from the mass balances over a volume element of the bed and inside the particle. Axial dispersion flow for the bulk fluid phase is included and the linear driving force (LDF) approximation is used to describe the intraparticle mass-transfer rate.

Mass balance over a volume element of the bed k for proteins and salt:

$$\frac{\partial C_{ik}}{\partial t} = D_{Lk}\frac{\partial^2 C_{ik}}{\partial Z^2} - \frac{u_k}{\varepsilon_B}\frac{\partial C_{ik}}{\partial Z} - \frac{(1-\varepsilon_B)}{\varepsilon_B}k_{Pik}[q^*_{ik} - q_{ik}] \quad (1)$$

Mass balance in the particles for proteins and salt described by LDF model:

$$\frac{\partial q_{ik}}{\partial t} = k_{Pik}(q^*_{ik} - q_{ik}) \quad (2)$$

where C is the concentration in the fluid phase; q is the average adsorbed phase concentration in adsorbent; q^* is the adsorbed phase concentration in equilibrium with the fluid phase concentration; Z is the axial distance from the column entrance; t is the time; ε_B is the bed voidage in column; u is the superficial velocity; D_L is the axial dispersion coefficient; k_P is the mass transfer coefficient; k refers to the column number, total N columns in the gradient SMB unit; and i refers to proteins and salt.

Initial conditions:

$$t = 0 : C_{ik} = q_{ik} = 0 \text{ for proteins} \quad (3a)$$

Before the feed is applied to the column, a salt gradient has been formed in the SMB unit as

$$C_{Sk} = C^D_S,\ q_{Sk} = q^*_{Sk}(C^D_S) \text{ in section I and II} \quad (3b)$$

$$C_{Sk} = C^F_S,\ q_{Sk} = q^*_{Sk}(C^F_S) \text{ in section III and IV} \quad (3c)$$

Boundary conditions in each column for proteins and salt:

$$D_{Lk}\varepsilon_B\left.\frac{\partial C_{ik}}{\partial Z}\right|_{Z=0} = u_k\left[C_{ik}\big|_{Z=0} - C_{ik,0}\right] \quad (4a)$$

$$\left.\frac{\partial C_{ik}}{\partial Z}\right|_{Z=L_k} = 0 \quad (4b)$$

Mass balances at nodes:

At the desorbent node,

$$C_{i1,0} = C_i^{\mathrm{D}} \text{ open loop} \tag{5a}$$

$$C_{i1,0} = \frac{Q_{\mathrm{D}} C_i^{\mathrm{D}} + Q_{\mathrm{rec}} C_{iN}\big|_{Z=L_N}}{Q_{\mathrm{I}}} \text{ closed loop} \tag{5b}$$

$$V_{\mathrm{S}} \frac{dC_{i1,0}}{dt} + Q_{\mathrm{I}} C_{i1,0} = Q_{\mathrm{D}} C_i^{\mathrm{D}} + Q_{\mathrm{rec}} C_{iN}\big|_{Z=L_N} \tag{5c}$$

closed loop with a holding vessel

The holding vessel has a constant volume V_{S} with initial condition of $C_{i1,0} = C_i^{\mathrm{D}}$ at $t = 0$.

At the extract node,

$$C_{ik+1,0} = C_{ik}\big|_{Z=L_k} \tag{5d}$$

At the feed node,

$$C_{ik+1,0} = \frac{Q_{\mathrm{F}} C_i^{\mathrm{F}} + Q_{\mathrm{II}} C_{ik}\big|_{Z=L_k}}{Q_{\mathrm{III}}} \tag{5e}$$

At the raffinate node,

$$C_{ik+1,0} = C_{ik}\big|_{Z=L_k} \tag{5f}$$

At the nodes between the other columns,

$$C_{ik+1,0} = C_{ik}\big|_{Z=L_k} \tag{5g}$$

Global balances:

$$Q_{\mathrm{I}} = Q_{\mathrm{D}} \text{ open loop} \tag{6a}$$

$$Q_{\mathrm{I}} = Q_{\mathrm{D}} + Q_{\mathrm{rec}} \text{ closed loop} \tag{6b}$$

$$Q_{\mathrm{II}} = Q_{\mathrm{I}} - Q_{\mathrm{E}} \tag{6c}$$

$$Q_{\mathrm{III}} = Q_{\mathrm{II}} + Q_{\mathrm{F}} \tag{6d}$$

$$Q_{\mathrm{IV}} = Q_{\mathrm{III}} - Q_{\mathrm{R}} \tag{6e}$$

where Q_{I}, Q_{II}, Q_{III}, Q_{IV} are the flow rates in sections I, II, III, and IV, respectively; Q_{D}, Q_{E}, Q_{F}, Q_{R}, and Q_{rec} are desorbent flow rate, extract flow rate, feed flow rate, raffinate flow rate, and recycle flow rate, respectively; C_i^{D} and C_i^{F} are component concentrations in desorbent and feed, respectively.

As a result of the switch of inlet and outlet lines, each column plays different functions during a whole cycle, depending on its location (section). As a consequence, the boundary conditions for each column change at the end of each switch time interval. When the cyclic steady state is reached, the internal concentration profiles vary during a given cycle, but they are identical at the same time for two successive cycles.

Model parameters and numerical method

The diffusivities[26] of BSA and myoglobin in water are $D_{\mathrm{BSA},0} = 6.15 \times 10^{-11}$ m^2/s and $D_{\mathrm{MYO},0} = 11.3 \times 10^{-11}$ m^2/s, respectively. The effective pore diffusivities[26] of BSA and myoglobin in Q-Sepharose FF resin are estimated as $D_{\mathrm{Pe,BSA}} = 1.5 \times 10^{-11}$ m^2/s, and $D_{\mathrm{Pe,MYO}} = 3.6 \times 10^{-11}$ m^2/s, here $D_{\mathrm{Pe},i} = \varepsilon_{\mathrm{P}i} D_{0,i/\tau}$ and tortuosity factor τ assigned as 2. The mass transfer coefficient[27] $k_{\mathrm{P}ik}$ in Eq. 2 is calculated by

$$k_{\mathrm{P}ik} = \frac{15 D_{\mathrm{Pe},i}}{(0.5 d_{\mathrm{P}})^2} \Big/ \frac{dq_{ik}}{dC_{ik}} \tag{7}$$

The mass transfer coefficient $k_{\mathrm{PS}k}$ for salt is higher, about 2.0 s^{-1}. When $k_{\mathrm{PS}k} \geq 0.5$ s^{-1}, the effect of $k_{\mathrm{PS}k}$ on the simulation results is negligible, so we set $k_{\mathrm{PS}k} = 0.5$ s^{-1} in order to quickly get a stable numerical solution.

The liquid axial dispersion coefficient $D_{\mathrm{L}k}$ is estimated by Chung and Wen correlation[28]:

$$D_{\mathrm{L}k} = \frac{d_{\mathrm{P}} u_k}{0.20 + 0.011 (d_{\mathrm{P}} u_k \rho / \mu)^{0.48}} \tag{8}$$

with $\rho = 1000$ kg/m^3 and $\mu = 0.89$ cP approximately taken as those of water.

The central finite difference method is used to discretize Eq. 1 in the axial direction in each column, leading to a set of ordinary differential equations with initial values; at these discretized points in each column, Eq. 2 is also represented as a set of ordinary differential equations with initial values. All ordinary differential equations will be solved together using Gear's stiff variable step integration routine. It should be noticed that the initial state in each column varies with switching interval if the column positions are fixed during the simulation.

Proteins and salt adsorption equilibrium isotherm on Q-Sepharose FF ion exchanger and adsorption kinetics

In the aforementioned gradient SMB model, the mass balance in the particles is described by the LDF model, so the amount of protein adsorbed on the ion exchange resin includes two terms: one is the protein IE amount with the ligand of adsorbent, and the other is the distribution amount in the accessible porosity (size exclusion) of adsorbent. When the salt concentration is high, the protein IE amount becomes weak, and the distribution amount in the accessible porosity will be important.

Protein IE equilibrium at various salt concentrations can be described by the steric mass action (SMA) model, which was developed by Brook and Cramer.[29] In the SMA model, ion exchange is regarded as a reaction of a characteristic number of charges of a protein with many salt ions bound to the ion-exchanger, and the protein IE equilibrium isotherm can be expressed as

$$C = \frac{q^{\mathrm{IE}} C_{\mathrm{S}}^z}{K\left[q_0 - (z+\sigma) q^{\mathrm{IE}}\right]^z} \text{ for single component protein} \tag{9}$$

and

$$C_i = \frac{q_i^{\mathrm{IE}} C_{\mathrm{S}}^{z_i}}{K_i\left[q_0 - \sum (z_i + \sigma_i) q_i^{\mathrm{IE}}\right]^{z_i}} \text{ for multicomponent proteins} \tag{10}$$

The parameters z, K, and σ should be measured by independent experiments, such as using the isocratic/gradient elution chromatography, recommended by Book and Cramer[29] and

Pedersen et al.[30] z is the characteristic charge representing the number of sites that the protein interacts with on the resin surface; K is the binding constant for the stoichiometric binding reaction between the protein and salt counterions; σ (steric factor) means the number of sites on the resin surface that are shielded by the protein and prevented from exchange. In the equations, q_0 (ionic or bed capacity) is the total number of binding sites available on the resin surface, usually provided by manufacturer, which can be measured as indicated by Whitley et al.[31]

Either for dilute protein solution or at high salt concentration, the protein IE amount q^{IE} is very small, that is $q_0 \gg (\sigma + z)q^{IE}$; then Eq. 9 becomes a linear ion exchange equilibrium isotherm:

$$q^{IE} = \frac{Kq_0^z}{C_S^z} C \tag{11}$$

Linear IE equilibria for BSA and myoglobin on Q-Sepharose FF resin (in 10 mM Tris buffer, pH 8) were reported by Houwing et al.[11] as

$$q^{IE}_{BSA} = 0.00161 C_S^{-5.61} C_{BSA} \tag{12a}$$

$$q^{IE}_{MYO} = 0.0761 C_S^{-1.31} C_{MYO} \tag{12b}$$

The accessible porosities of BSA and myoglobin in Q-Sepharose FF are 0.49 and 0.64, respectively, measured by Houwing et al.,[11] so the adsorption equilibrium isotherm of BSA and myoglobin on Q-Sepharose FF can be expressed as

$$q^*_{BSA} = (0.49 + 0.00161 C_S^{-5.61}) C_{BSA} \tag{13a}$$

$$q^*_{MYO} = (0.64 + 0.076 C_S^{-1.31}) C_{MYO} \tag{13b}$$

where C_S is the salt concentration (expressed in M).

IE equilibrium isotherms of BSA and myoglobin on Q-Sepharose FF resin were studied experimentally in our laboratory over a wide protein concentration range, as shown in Figure 3. Equilibrium data were measured in a static batch adsorber. Before performing the protein ion exchange equilibrium experiments, the resins must be saturated with the corresponding buffer. Resins, in the amount of 0.5–2.5 mL of particle volume, are equilibrated with 30 mL of different

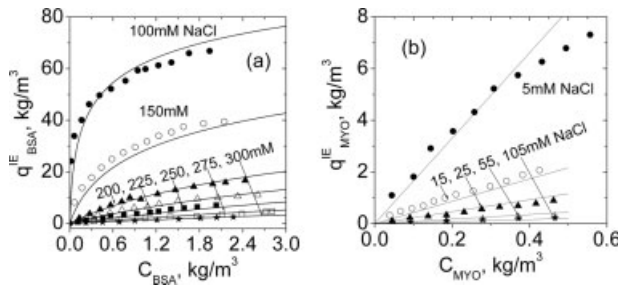

Figure 3. Ion exchange equilibrium isotherms of BSA and myoglobin on Q-Sepharose FF resin in pH 8 Tris buffer (10 mM), at room temperature (~25°C).

Symbols: experimental data; lines: calculated using Eq. 14 for BSA and Eq. 15 for myoglobin.

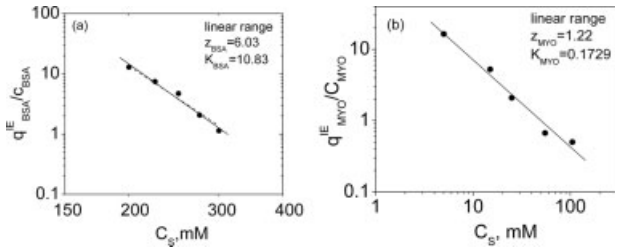

Figure 4. Plots of $\log(q_i^{IE}/C_i)$ versus $\log(C_S)$ in the linear ion exchange equilibrium isotherm.

Symbols: experimental data taken from Figure 3; solid lines: the linear regression lines; dashed line: calculated using Eq. 12a.

concentrations of BSA or myoglobin solution for 20 h at 25°C on a shaking incubator (about 30 rpm); then BSA or myoglobin concentration in supernatant liquid are measured by UV 7800 detector at 280 nm (using a 2-mL quartz cuvette). The ion exchange capacity is calculated by the mass balance ($q_i^{IE} = V_L^*(C_{i0} - C_i)/V_S^* - \varepsilon_{Pi}C_i$). Here, the corresponding buffer is 10 mM Tris buffer (pH 8) with different NaCl concentrations. BSA product number is A3059 and myoglobin product number is M0630, both from Sigma-Aldrich Company.

BSA has a high ion exchange capacity on Q-Sepharose FF resin at pH 8 Tris buffer (10 mM), with a high favorable nonlinear equilibrium isotherm, because the isoelectric point (pI 4.7) of BSA is far from the buffer pH value (pH 8). The ion exchange equilibrium isotherm of BSA on Q-Sepharose FF resin with the dependence on NaCl concentration can be represented by the SMA model as

$$C_{BSA} = \frac{q^{IE}_{BSA} C_S^{z_{BSA}}}{K_{BSA}\left[q_0 - (z_{BSA} + \sigma_{BSA}) q^{IE}_{BSA}/M_{BSA}\right]^{z_{BSA}}} = \frac{q^{IE}_{BSA} C_S^{6.03}}{10.83\left[0.210 - (6.03 + 75) q^{IE}_{BSA}/M_{BSA}\right]^{6.03}} \tag{14}$$

where q^{IE}_{BSA} and C_{BSA} are expressed in kg/m^3, C_S in M, and M_{BSA} is BSA molecular weight (65400), q_0 = 0.21 M for Q-Sepharose FF resin at pH 8 buffer measured by Whitley et al.[31] The model parameters, z_{BSA} = 6.03 and K_{BSA} = 10.83, are estimated from the plot of $\log(q^{IE}_{BSA}/C_{BSA})$ versus $\log(C_S)$ with the slope of z_{BSA}, and intercept equal to $\log(K_{BSA}q_0^{z_{BSA}})$ under linear IE equilibrium isotherms, as shown in Figure 4a; experimental data are taken from Figure 3a for linear cases [IE for diluted BSA solutions at high salt concentrations (200–300 mM NaCl)]. The other model parameter, σ_{BSA} = 75, is measured by fitting the nonlinear IE equilibrium data with Eq. 14 at various salt concentrations, and then an average value over the range of salt concentrations is assigned to σ_{BSA}. The predicted values by Eq. 14 are close to the experimental results at various salt concentrations, as shown in Figure 3a.

Since the pH value (pH 8) in 10 mM Tris buffer approaches the isoelectric point of myoglobin (pI 7.4), the ion exchange amount of myoglobin on Q-Sepharose FF resin is very small even at low salt concentration. Over a wide myoglobin concentration range, the linear ion exchange equi-

librium isotherms can be found at different NaCl concentrations. Based on the experimental results shown in Figure 3b, the linear IE equilibrium isotherm of myoglobin on Q-Sepharous FF resin is expressed as

$$q_{\mathrm{MYO}}^{\mathrm{IE}} = \frac{K_{\mathrm{MYO}} q_0^{z_{\mathrm{MYO}}}}{C_{\mathrm{S}}^{z_{\mathrm{MYO}}}} C_{\mathrm{MYO}} = 0.02576 C_{\mathrm{S}}^{-1.22} C_{\mathrm{MYO}} \qquad (15)$$

where $q_{\mathrm{MYO}}^{\mathrm{IE}}$ and C_{MYO} are expressed in kg/m^3, C_{S} in M, and $q_0 = 0.21$ M. The model parameters, $z_{\mathrm{MYO}} = 1.22$ and $K_{\mathrm{MYO}} = 0.1729$, are estimated from the plot of $\log(q_{\mathrm{MYO}}^{\mathrm{IE}}/C_{\mathrm{MYO}})$ versus $\log(C_{\mathrm{S}})$ for linear IE equilibrium isotherms, as shown in Figure 4b. The predicted values by Eq. 15 are close to the experimental results at various salt concentrations, as shown in Figure 3b.

Furthermore, breakthrough curves of BSA and myoglobin are measured in a fixed bed, as shown in Figure 5a–c, where XK16/20 column is packed with Q-Sepharose FF anion exchangers, packed height 100 mm, column diameter 16 mm, bed voidage 0.35 (estimated from a given mass of drained resins to pack the column, drained resins with 1050 kg/m^3 density). The experimental data of breakthrough curves are compared with the simulation results in Figure 5, to confirm the accuracy of ion exchange equilibrium isotherm expressions (Eq. 14 for BSA and Eq. 15 for myoglobin). The mass transfer coefficients $k_{\mathrm{P}i}$ of BSA and myoglobin are evaluated by fitting the experimental data of breakthrough curves with the LDF model. For myoglobin with linear adsorption isotherm, k_{PMYO} can be calculated by Eq. 7 with $D_{\mathrm{Pe,MYO}} = 3.0 \times 10^{-11}$ m^2/s; for BSA at 300 and 200 mM NaCl buffer, k_{PBSA} can be calculated using Eq. 7 with $D_{\mathrm{Pe,BSA}} = 1.5 \times 10^{-11}$ m^2/s, $k_{\mathrm{PBSA}} = 0.00278$ s^{-1} at 150 mM NaCl and $k_{\mathrm{PBSA}} = 0.00139$ s^{-1} at 100 mM NaCl. Moreover, as commonly observed by many authors, there exist a severe tailing behavior of BSA breakthrough curve as the effluent approaches the feed concentration. In previously published articles,[27,32,33] the tailing behavior was explained by the presence of dimer in BSA sample, or microporous diffusion in the macroporous adsorbent, or protein aggregation into dimer or trimer on the adsorbed surface of adsorbents. Up to now, the explanation of the tailing behavior for the adsorption of larger protein molecule is still unclear.

The salt adsorption equilibrium on Q-Sepharose FF resin is expressed as

$$q_{\mathrm{s}} = 0.22\left(-0.5 + 0.5\sqrt{1 + 4\times 1.09 \times C_{\mathrm{S}}^2/0.22^2}\right)$$
$$= 0.11\left(-1 + \sqrt{1 + 90.083 C_{\mathrm{S}}^2}\right) \qquad (16)$$

according to Houwing et al.,[34] and salt concentration C_{S} in M.

Results and Discussion

Transient concentration profiles formed in salt gradient IE-SMB

Houwing et al.[11] reported experimental results for the separation of BSA and myoglobin by salt gradient IE-SMB chromatography; operating conditions and SMB configuration are shown in Table 1. The salt gradient was formed in the IE-SMB chromatography by introducing feed with a lower salt concentration (0.15 M NaCl) and desorbent with a higher salt concentration (0.27 M NaCl). When the feed with BSA and myoglobin was applied to the salt gradient IE-SMB, the weakly retained component, myoglobin was eluted with the raffinate stream, and the large BSA molecule was eluted from the extract stream as a strongly retained component. Their experimental results confirmed qualitatively that BSA and myoglobin can be separated efficiently by the salt gradient IE-SMB chromatography.

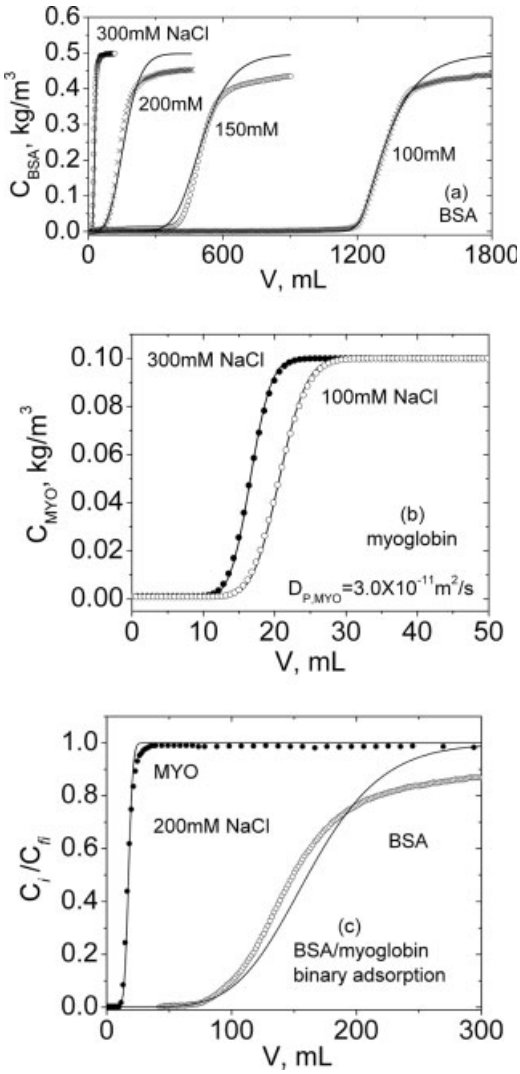

Figure 5. BSA and myoglobin breakthrough curves at various NaCl concentrations.

Circles: experimental data; lines: simulation results with LDF model. (a) Single component breakthrough curve for BSA. $Q = 7.2$ mL/min (100 mM NaCl), $Q = 7.0$ mL/min (150 mM NaCl), $Q = 7.0$ mL/min (200 mM NaCl), $Q = 3.5$ mL/min (300 mM NaCl). (b) Single component breakthrough curve for myoglobin. $Q = 4.0$ mL/min (100 mM NaCl) and $Q = 4.75$ mL/min (300 mM NaCl). (c) Binary breakthrough curves BSA/MYO. $Q = 4.9$ mL/min (200 mM NaCl), $C_{\mathrm{f,BSA}}/C_{\mathrm{f,MYO}} = 0.5$ kg/m^3/0.1 kg/m^3.

Figures 6–8 show a series of the transient concentration profiles formed in the salt gradient IE-SMB, which are calculated by the gradient SMB model based on the experimental conditions and configuration listed in Table 1, to demonstrate

Table 1. Configuration and Experimental Conditions for BSA and Myoglobin Separation by Salt Gradient Ion-exchange SMB

Configuration	Feed Composition	Desorbent Composition	Flow Rates (mL/min)
Open loop 2-2-2-2; switch time 4.182 min, columns packed with Q-Sepharose FF resin, column diameter 10 mm, packed height 90.4 mm, bed voidage 0.39	$C_S^F = 0.15$ M, $C_{BSA}^F = 0.5$ kg/m^3, $C_{MYO}^F = 0.1$ kg/m^3	$C_S^D = 0.27$ M	$Q_D = 2.94$, $Q_E = 1.03$, $Q_F = 2.02$, $Q_R = 2.05$

Experimental results shown in Figure 6 of the literature.[11]

the process of the salt gradient formation and the efficient separation process of BSA and myoglobin by salt gradient IE-SMB. The adsorption equilibrium isotherm of proteins reported by Houwing et al.[11] are linear (Eqs. 13a and 13b). It is not clear from the work reported by Houwing et al.[11] which is the protein concentration of the feed. Here we estimate the feed with 0.5 kg/m^3 BSA and 0.1 kg/m^3 myoglobin during the simulation. Since this is linear adsorption, the absolute concentration levels of the proteins are irrelevant to the operation conditions.

Figure 6 shows the cases in the first full cycle (switch 8 times), where the transient concentration profiles before next switch are shown successively from the initial state in salt gradient IE-SMB. Before feed is applied to the column, the salt gradient in IE-SMB has been formed by introducing the corresponding salt solutions to the columns, as shown in Figure 6 for the case with $t = 0$. Then the feed with BSA (0.5 kg/m^3), myoglobin (0.1 kg/m^3), and salt (0.15 M NaCl) is introduced to the column in section III, and the desorbent with 0.27 M NaCl is simultaneously applied to the column in section I to desorb the bound proteins. With the switch of inlet and outlet lines, the strongly retained component BSA moves gradually downward to the extract port, and the weakly retained component myoglobin moves gradually upward to the raffinate port, as shown in Figure 6. The salt gradient will redistribute dynamically according to the salt concentrations in feed and desorbent and switch frequency.

After 10 cycles (about switch 80 times), a cyclic steady state can be reached, as shown in Figure 7, where concentration profiles at half switch time are almost identical for two successive cycles. Salt gradient is formed easily in IE-SMB and reaches quickly the cyclic steady state. The internal concentration profile for the weakly retained component myoglobin quickly reached the cyclic steady state also. However, it takes more than 10 cycles to reach the cyclic steady state for the BSA concentration profile.

After the cyclic steady state is reached, the concentration profiles at the end of a switch time interval are the same as at the beginning of this interval, but they are advanced one column. These profiles will be reproduced in the same way column after column. A typical evolution of the internal concentration profiles during a switch time interval at the cyclic steady state (20 cycles), is shown in Figure 8.

When comparing the simulation results with the experimental data reported by Houwing et al.[11] (shown in Figure 6),[11] it was found that the internal concentration profiles of salt and

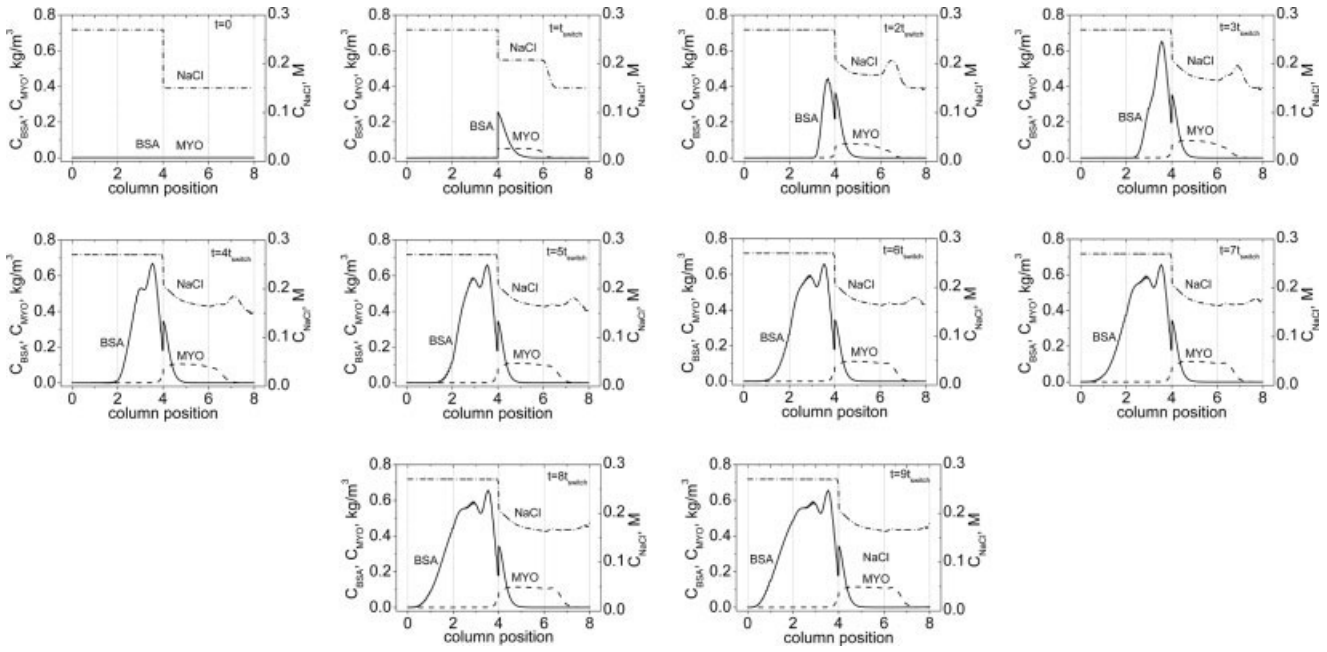

Figure 6. Transient concentration profiles before next switch in salt gradient IE-SMB with open loop in the first full cycle, operating conditions for the simulations shown in Table 1.

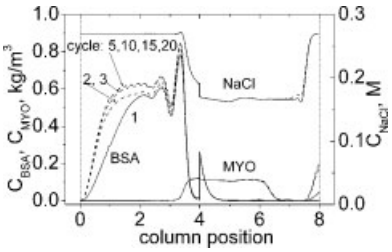

Figure 7. Concentration profiles at half switch time with different cycles in salt gradient IE-SMB with open loop, operating conditions for the simulations shown in Table 1.

myoglobin at half switch time calculated by the gradient SMB model agree reasonably with the experimental results, but a deviation is found for the internal concentration profile of BSA, where the simulation results are higher than the experimental data. From the global BSA mass balance, it seems that the cyclic steady state was not reached for BSA if BSA concentration in feed was 0.5 kg/m^3 in this experiment. As shown in Figure 7, it takes more than 10 cycles to reach the cyclic steady state for BSA concentration profile. The other explanation for the BSA profile deviation is the reequilibrium limitation of BSA and salt in sections I and II as a result of the short switch time interval during experiments, suggested by one reviewer.

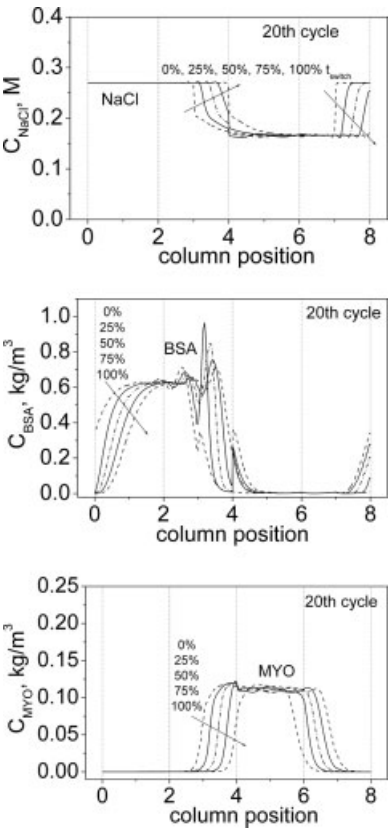

Figure 8. Cyclic steady state internal concentration profiles during a switch time interval in salt gradient IE-SMB with open loop, operating conditions for the simulations shown in Table 1.

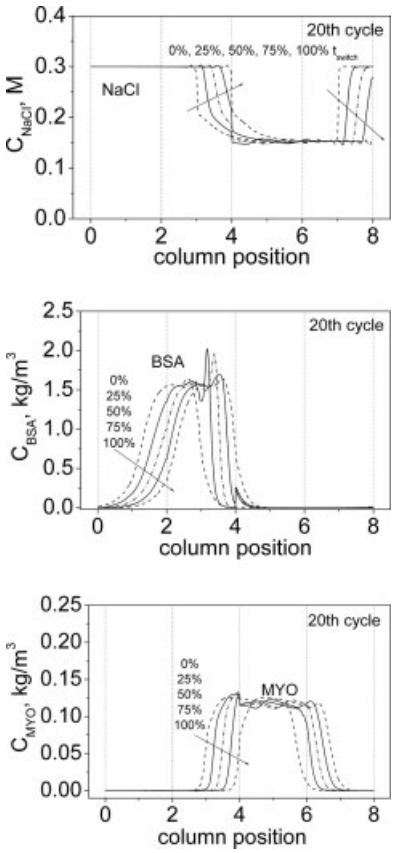

Figure 9. Cyclic steady state internal concentration profiles during a switch time interval in salt gradient IE-SMB with open loop, C_S^D = 0.3 M and C_S^F = 0.13 M and other operating conditions for simulations shown in Table 1.

In the gradient SMB model, we assume the reequilibrium of proteins and salt attainted instantaneously.

Moreover, poor regeneration of adsorbents is found in section I. Since the BSA IE amount is sensitive to the salt concentration in the buffer, a simple and easy method to improve the regeneration of the adsorbent in section I is to increase the salt concentration in the desorbent. Figure 9 shows the simulation results when the salt concentration is increased to 0.3 M NaCl in desorbent, and the salt concentration in the feed is adjusted correspondingly as 0.13 M NaCl in order to keep similar separation in sections III and IV as before (Figure 8). As shown in Figure 9, the adsorbent in section I can indeed be regenerated very well, there is almost no loss of BSA in the effluent stream from section IV, and the BSA average concentration in the extract stream can be increased to 1 kg/m^3. Enrichment of BSA in the extract stream up to 2 means BSA is concentrated relative to the feed flow during separation. Enrichment is defined as

$$E_i = \frac{C_i^E}{C_i^F} \text{ in extract stream} \tag{17a}$$

$$E_i = \frac{C_i^R}{C_i^F} \text{ in raffinate stream} \tag{17b}$$

Table 2. Operating Conditions for the Simulations and Configurations of Salt Gradient Ion-exchange SMB

	Run A	Run B	Run C
Configuration	Open loop, 2-2-2-2	Closed loop, 2-2-2-2	Closed loop with a holding vessel, (V_S = 10 mL), 2-2-2-2
Feed composition	C_S^F = 0.13 M C_{BSA}^F = 0.3 kg/m^3 C_{MYO}^F = 0.1 kg/m^3	C_S^F = 0.13 M C_{BSA}^F = 0.3 kg/m^3 C_{MYO}^F = 0.1 kg/m^3	C_S^F = 0.13 M C_{BSA}^F = 0.3 kg/m^3 C_{MYO}^F = 0.1 kg/m^3
Desorbent composition (M)	C_S^D = 0.30	C_S^D = 0.34	C_S^D = 0.34
Flow rates (mL/min)	Q_D = 2.94 Q_E = 1.03 Q_F = 2.02 Q_R = 2.05 Q_{rec} = 0	Q_D = 1.06 Q_E = 1.03 Q_F = 2.02 Q_R = 2.05 Q_{rec} = 1.88	Q_D = 1.06 Q_E = 1.03 Q_F = 2.02 Q_R = 2.05 Q_{rec} = 1.88
Switch time (min)	4.182	4.182	4.182

Columns packed with Q-Sepharose FF anion exchangers, column diameter 10 mm, column packed height 90.4 mm, bed voidage 0.39 (reference to the design done by Houwing et al.[11]).

In the raffinate stream, the myoglobin average concentration is about 0.1 kg/m^3, not diluted relative to the feed flow. The enrichment of protein concentration in the extract stream is a significant improvement in gradient SMB when compared with isocratic SMB. However, the local protein concentrations are high in section II in the salt gradient SMB unit, which would cause precipitation if a protein has a lower solubility in the solution with medium or high salt concentration.

With the increase of salt concentration to 0.3 M in desorbent, the local concentration of BSA in section II becomes very high; the simulation with the linear IE equilibrium isotherm would result in deviation from the actual process. Based on our experimental results, with 0.3 M NaCl in buffer, over a wide BSA concentration range (0–3 kg/m^3), IE equilibrium isotherm of BSA on Q-Sepharose FF resin is still linear. But in sections II and III of the gradient SMB unit, there exist lower salt concentration zone for adsorption and desorption of high concentration BSA, where the linear IE equilibrium isotherm is not valid. Therefore, the nonlinear IE equilibrium isotherm should be considered.

Comparison of gradient SMB configurations: open loop, closed loop, and closed loop with a holding vessel

The detailed operating conditions for three configurations of gradient SMB are listed in Table 2, open loop (Run A), closed loop (Run B), and closed loop with a holding vessel (Run C). In the case of open loop, desorbent with 0.3 M NaCl is applied to the columns at 2.94 mL/min flow rate; for closed loop, desorbent flow rate can be decreased to 1.06 mL/min because of the recycle of liquid from section IV, but the salt concentration should be increased to 0.34 M NaCl in desorbent to keep the similar salt gradient in columns of SMB unit. The simulation results at the cyclic steady state (20 cycles) are shown in Figures 10 (open loop), 11 (closed loop), and 12 (closed loop with a holding vessel V_S = 10 mL), respectively. Here, BSA concentration in feed is assigned as 0.3 kg/m^3, instead of 0.5 kg/m^3 used before, and the linear adsorption equilibrium isotherms of BSA and myoglobin (Eqs. 13a and 13b) are used in simulations.

In open loop, as shown in Figure 10, in the positions of column 4 of section II and column 8 of section IV, salt concentrations dynamically vary during a switch time interval. The direct recycling of liquid stream from section IV to section I in closed loop, will cause the dynamic change of salt concentration in section I also, as shown in Figure 11, where the salt concentration decreases gradually and makes the adsorbent regeneration inefficient in section I. When a holding vessel with 10 mL volume (about 1.5 column volume) is used to mix online the desorbent with the recycled stream from section IV before applied to column 1 in section I in closed loop, as shown in Figure 12, the dynamic change of salt concentration in section I during a switch time interval is indeed weak, which favors the adsorbent regeneration in section I.

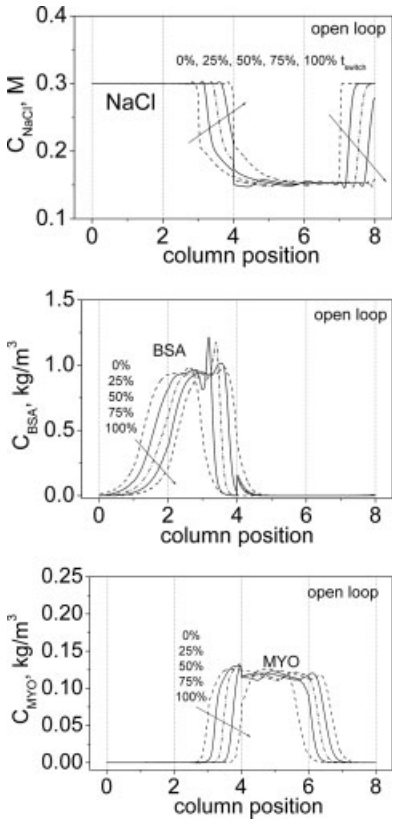

Figure 10. Internal concentration profiles at cyclic steady state (20 cycles) in salt gradient IE-SMB with open loop, operating conditions for the simulations shown in Table 2 (Run A)

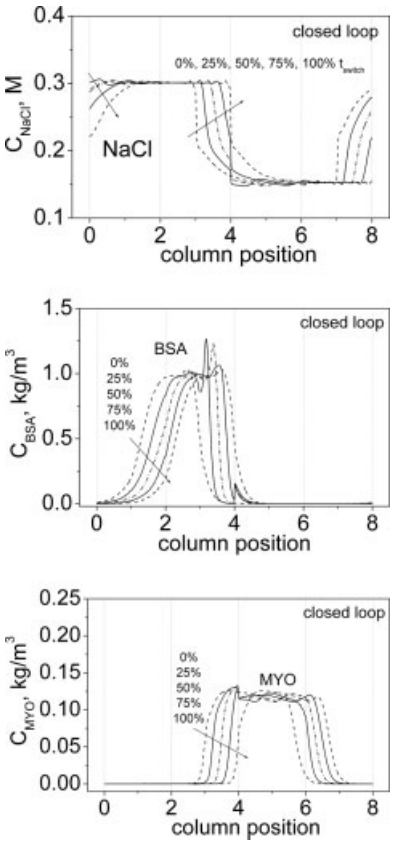

Figure 11. Internal concentration profiles at cyclic steady state (20 cycles) in salt gradient IE-SMB with closed loop, operating conditions for the simulations shown in Table 2 (Run B).

Here, similar salt gradients are formed in open loop, closed loop, and closed loop with a holding vessel at given operating conditions (Table 2); BSA and myoglobin can be separated with almost identical efficiency by the three kinds of configurations of gradient SMB.

Comparison of the two strategies of modeling, gradient SMB/gradient TMB model

Two models are frequently used to simulate an SMB unit: one is the true moving bed (TMB) model, which assumes equivalence with an ideal unit where the solid and the liquid phases move countercurrently; the other is the SMB model, where the dynamics associated with the periodic shift of the inlet and outlet lines is taken into account. It is known that the prediction of the isocratic SMB operation can be carried out through the equivalent isocratic TMB approach when the SMB unit is constituted by, at least, two columns per section (a total of eight columns). Here, we will present the comparison of the two strategies of modeling, gradient SMB model, and equivalent gradient TMB model for predicting internal concentration profiles in gradient SMB chromatography.

Figure 13 demonstrates the internal concentration profiles at steady state in salt gradient IE-SMB with open loop and closed loop, respectively, predicted by the equivalent gradient TMB model. The mathematical model equations for the equivalent gradient TMB model are given in the Appendix. Operating conditions are identical to those in Figure 10 for the corresponding open loop predicted with the gradient SMB model, and to those in Figure 11 for the corresponding closed loop predicted with the gradient SMB model, respectively. The salt gradient formed in IE-SMB chromatography, i.e., in sections I and II with higher salt concentration and in sections III and IV with lower salt concentration, are identical when predicted by the gradient SMB model and by the gradient TMB model. However, the actual dynamical changes of salt concentrations in the positions of column 4 in section II and column 8 in section IV, and column 1 in section I (in particular for the closed loop) cannot be predicted by the gradient TMB model; also the corresponding significant change in BSA concentration cannot be represented by the gradient TMB model. It seems that the deviation between the predictions by the gradient SMB model and gradient TMB model becomes small for the weakly retained myoglobin, as a result of the small effect of salt concentration on myoglobin ion exchange amount. From the point of view of global mass balance of BSA, myoglobin and salt in salt gradient IE-SMB chromatography, when two proteins can be separated completely, protein concentrations in extract and raffinate predicted by two models should be identical, so

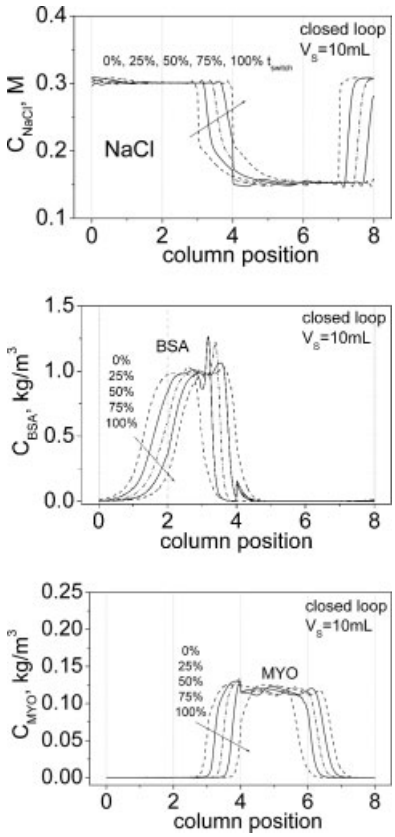

Figure 12. Internal concentration profiles at cyclic steady state (20 cycles) in salt gradient IE-SMB with closed loop and a holding vessel (V_S=10 mL), operating conditions for the simulations shown in Table 2 (Run C).

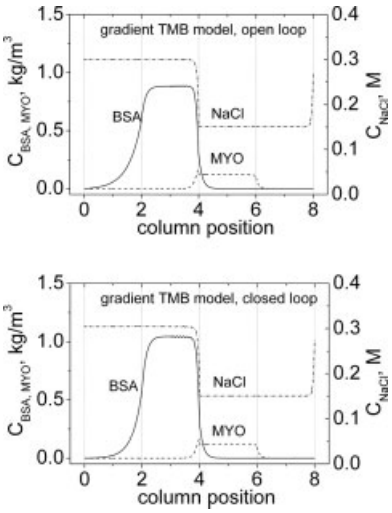

Figure 13. Internal concentration profiles at the steady state in salt gradient IE-SMB with open loop and closed loop, respectively, predicted by the gradient TMB model.

Operating conditions for simulations are identical with Figure 10 (open loop, predicted by the gradient SMB model) and Figure 11 (closed loop, predicted by the gradient SMB model).

as primary design of the gradient SMB chromatography, the simple gradient TMB model is applicable, because it can save computer time for the selection and optimization of flow rates in each section.

Strategies for the selection of salt gradient in IE-SMB chromatography

The separation factor is defined as

$$S_{1,2} = \frac{q_1/C_1}{q_2/C_2} \tag{18}$$

Table 3 lists the separation factors of BSA/myoglobin by Q-Sepharose FF anion exchanger at various salt concentrations, estimated approximately based on linear adsorption isotherms for BSA and myoglobin over 200–300 mM NaCl range (taken from Eqs. 14 and 15).

$$q^*_{\mathrm{BSA}} = K_{\mathrm{BSA}} C_{\mathrm{BSA}} = (0.49 + 8.8636\times10^{-4} C_{\mathrm{S}}^{-6.03}) C_{\mathrm{BSA}} \tag{19}$$

$$q^*_{\mathrm{MYO}} = K_{\mathrm{MYO}} C_{\mathrm{MYO}} = (0.64 + 0.02576 C_{\mathrm{S}}^{-1.22}) C_{\mathrm{MYO}} \tag{20}$$

Results in Table 3 show that the separation factor of these proteins depends evidently on salt concentration in Tris buffer. When NaCl concentration in Tris buffer (pH 8) is lower, the separation factor is larger; for example, with 200 mM NaCl in Tris buffer, $S_{\mathrm{BSA,MYO}}$ is 18.24, BSA and myoglobin can be separated easily by IEC. With the increase of salt concentration, the separation factor becomes significantly smaller. When salt concentration is up to 400 mM NaCl, the separation factor approaches 1, which means BSA and myoglobin cannot be separated by IEC. This phenomena is called azeotrope.[35] By increasing further the salt concentration, a reversal of separation is found, that is myoglobin becomes the more retained component and BSA becomes the less retained component, and the separation behavior of BSA and myoglobin in IEC is more close to that in SEC.

A step-wise salt gradient can be formed easily in IE-SMB packed with Q-Sepharose FF resin by introducing the feed with lower salt concentration and the desorbent with higher salt concentration. The lower salt concentration formed in sections III and IV will favor the separation of BSA and myoglobin as a result of the high separation factor. During the design, we assign salt concentration less than 0.2 M in sections III and IV; with the high separation factor, the separation of BSA and myoglobin becomes easy in section III, and a high feed throughput can be performed. In sections I and II of the IE-SMB unit, the higher salt concentration is formed to desorb efficiently BSA and myoglobin molecules adsorbed on Q-Sepharose FF resin in order to reduce the desorbent consumption; however, salt concentration should be less than 350 mM NaCl, as a result of the significant decrease of the separation factor in section II.

Conclusions

Based on theoretical analysis, it is demonstrated that the separation and purification of proteins can be performed effectively by salt gradient IE-SMB chromatography. Although the experimental work done by Houwing and coworkers[11] confirmed qualitatively the potential application of proteins separation by salt gradient IE-SMB, further experimental validation is still necessary.

The selection of salt gradient is a key issue and is also flexible in the design of proteins separation and purification by salt gradient IE-SMB chromatography. In sections I and II of IE-SMB, a high salt concentration is assigned to desorb the bound

Table 3. Separation Factor of BSA to Myoglobin by Q-Sepharose FF Anion Exchanger under the Linear Adsorption Equilibrium Isotherm

Salt Concentration in pH 8 Tris Buffer (10 mM)	K_{BSA}	K_{MYO}	$S_{\mathrm{BSA,MYO}}$	Comments
200 mM NaCl	15.024	0.824	18.24	BSA: the more retained; Myoglobin: the less retained
250 mM NaCl	4.275	0.780	5.48	BSA: the more retained; Myoglobin: the less retained
300 mM NaCl	1.751	0.752	2.33	BSA: the more retained; Myoglobin: the less retained
350 mM NaCl	0.988	0.733	1.35	BSA: the more retained; Myoglobin: the less retained
400 mM NaCl	0.712	0.719	0.99	Azeotrope
500 mM NaCl	0.548	0.700	0.78	Myoglobin: the more retained; BSA: the less retained; Similar to size exclusion SMB

proteins on ion exchangers in order to reduce the desorbent consumption, but one should avoid using too high salt concentration, as a result of the significant decrease of separation factor in section II, and also because sometimes salt concentration may be limited by the proteins solubility. In sections III and IV, a lower salt concentration is assigned to increase adsorption of proteins, but for the case of protein purification from some impurities, the salt concentration should be raised a little to decrease the adsorption of impurities and contaminants on ion exchangers. Moreover, when the gradient SMB is run in closed loop to further reduce solvent consumption, it is better that a holding vessel with a given volume is added to the system to mix online the desorbent with the recycled liquid stream from section IV during switching interval, in order to reduce solvent strength fluctuation in section I.

Although it is known that the prediction of the isocratic SMB operation can be performed through the equivalent isocratic TMB approach when the SMB unit is constituted by, at least, two columns per section, some deviation is found between predictions from the gradient SMB model and the equivalent gradient TMB model. When the simple gradient TMB model is used to optimize flow rates in each section for the desired separation and purification of proteins by salt gradient IE-SMB chromatography, results must de used with caution.

Acknowledgments

We acknowledge financial support from *Fundação para a Ciência e a Tecnologia* (FCT grant SFRH/BD/6762/2001). We thank the reviewers for their helpful and stimulating criticism and suggestions.

Notation

C = concentration in the fluid, kg/m^3
$D_{i,0}$ = diffusivities of proteins and salt in water (m^2/s).
D_L = axial dispersion coefficient (m^2/s)
d_P = particle diameter (m)
D_{Pe} = effective pore diffusivity in adsorbent (m^2/s)
E_i = Enrichment, defined by Eq. 17
K = binding constant in SMA model
k_P = mass transfer coefficient (s^{-1})
L_C = column packed length (m)
q = average adsorbed concentration in adsorbent, kg/m^3 particle
q^* = adsorbed concentration in equilibrium with fluid concentration (kg/m^3)
q_0 = total ionic capacity of ion exchanger (mmol Cl^{-1}/mL particle for anion exchanger)
Q = volumetric liquid flow rate (m^3/s)
Q_S = solid volumetric flow rate (m^3/s), $Q_S = (1 - \varepsilon_B)V_C/t_{switch}$
$S_{1,2}$ = separation factor, defined by Eq. 18
t = time (s)
t_{switch} = switch time (s)
u = superficial liquid flow velocity (m/s)
u_S = solid flow velocity (m/s), $u_s = L_C/t_{switch}$
V_C = the column packed volume (m^3)
V_L^* = the solution volume in batch experiment (m^3)
V_S = volume of the holding vessel (m^3)
V_S^* = the adsorbents volume in batch experiment (m^3)
z = characteristic charge in SMA model
Z = axial distance from the column entrance (m)
σ = steric factor in SMA model
ε_B = bed voidage in column (m^3/m^3)
ε_P = particle porosity of adsorbent (m^3/m^3)
τ = tortuosity factor in pore of adsorbent

Subscripts and superscripts

I, II, III, IV = section I, section II, section III, and section IV in SMB unit
D, E, F, R, rec = desorbent, extract, feed, raffinate, and recycle
IE = ion exchange
N = total columns in SMB unit
SMB = simulation moving bed
TMB = true moving bed
i = components, BSA, myoglobin, and NaCl
j = section in SMB unit
k = column number
S = salt, NaCl
0 = inlet, initial

Literature Cited

1. Broughton DB. Production-scale adsorptive separations of liquid mixtures by simulated moving bed technology. *Sep Sci Technol.* 1984;19:723–736.
2. Ruthven DM, Ching CB. Countercurrent and simulated countercurrent adsorption separation processes. *Chem Eng Sci.* 1989;44:1011–1038.
3. Ma, Z., and Wang, NHL. Standing wave analysis of SMB chromatography: linear system. *AIChE J.* 1997;43:2488–2508.
4. Mazzotti M, Storti G, Morbidelli M. Optimal operation of simulated moving bed units for nonlinear chromatographic separations. *J Chromatogr A.* 1997;769:3–24.
5. Rodrigues AE, Pais LS. Design of SMB chrial separations using the concept of separation volume. *Sep Sci Technol.* 2004;39:245–270.
6. Pais LS, Loureiro JM, Rodrigues AE. Separation of 1,1′-bi-2-naphthol enantiomers by continuous chromatography in simulated moving bed. *Chem Eng Sci.* 1997;52:245–257.
7. Juza M, Mazzotti M, Morbidelli M. Simulated moving-bed chromatography and its application to chirotechnology. *Trends Biotechnol.* 2000;18:108–118.
8. Ludemann-Hombourger Q, Pigorini G, Nicoud RM, Ross DS, Terfloth G. Application of the VARICOL process to the separation of the isomers of the SB-553261 racemate. *J Chromatgr A.* 2002;947: 59–68.
9. Gottschlich N, Kasche V. Purification of monoclonal antibodies by simulated moving-bed chromatography. *J Chromatogr A.* 1997;765: 201–206.
10. Imamoglu S. Simulated moving bed chromatography (SMB) for application in bioseparation. *Adv Biochem Eng/Biotechnol.* 2002;76: 211–231.
11. Houwing J, van Hateren SH, Billiet HAH, van der Wielen LAM. Effect of salt gradients on the separation of dilute mixtures of proteins by ion-exchange in simulated moving beds. *J Chromatogr A.* 2002;952:85–98.
12. Xie Y, Mun S, Kim J, Wang NHL. Standing wave design and experimental validation of a tandem simulated moving bed process for insulin purification. *Biotechnol Process.* 2002;18:1332–1344.
13. Paredes G, Mazzotti M, Stadler J, Makart S, Morbidelli M. SMB operation for three-fraction separations: purification of plasmid DNA. *Adsorption.* 2005;11:841–845.
14. Geisser A, Hendrich T, Boehm G, Stahl B. Separation of lactose from human milk oligosaccharides with simulated moving bed chromatography. *J Chromatogr A.* 2005;1092:17–23.
15. Andersson J, Mattiasson B. Simulated moving bed technology with a simplified approach for protein purification—separation of lactoperoxidase and lactoferrin from whey protein concentrate. *J Chromatogr A.* 2006;1107:88–95.
16. Paredes G, Makart S, Stadler J, Makart S, Mazzotti M. Simulated moving bed operation for size exclusion plasmid purification. *Chem Eng Technol.* 2005;28:1335–1345.
17. Houwing J, Billiet HAH, van der Wielen LAM. Mass-transfer effects during separation of proteins in SMB by size exclusion. *AIChE J.* 2003;49:1158–1167.
18. Jensen TB, Reijns TGP, Billiet HAH, van der Wielen LAM. Novel simulated moving-bed method for reduced solvent consumption. *J Chromatogr A.* 2000;873:149–162.
19. Abel S, Babler MU, Arpagaus C, Mazzotti M, Stadler J. Two-fraction and three-fraction continuous simulated moving bed separation of nucleosides. *J Chromatogr A.* 2004;1043:201–210.
20. Abel S, Mazzotti M, Morbidelli M. Solvent gradient operation of simulated moving beds I. Linear isotherms. *J Chromatogr A.* 2002; 944:23–39.

21. Abel S, Mazzotti M, Morbidelli M. Solvent gradient operation of simulated moving beds —2. Langmiur isotherms. *J Chromatogr A*. 2004; 1026:47–55.
22. Antos D, Seidel-Morgenstern A. Application of gradients in the simulated moving bed process. *Chem Eng Sci*. 2001;56:6667–6682.
23. Antos D, Seidel-Morgenstern A. Two-step solvent gradients in simulated moving bed chromatography-numerical study for linear equilibria. *J Chromatogr A*. 2002;944:77–91.
24. Ziomek G, Kaspereit M, Jezowski JJ, Seidel-Morgenstern A, Antos D. Effect of mobile phase composition on the SMB processes efficiency stochastic optimization of isocratic and gradient operation. *J Chromatogr A*. 2005;1070:111–124.
25. Jensen TB. *Gradient SMB chromatography*. Ph.D thesis, Kluyver Laboratory for Biotechnology, Delft University of Technology, 2003.
26. Boyer PM, Hsu JT. Experimental studies of restricted protein diffusion in an agarose matrix. *AIChE J*. 1992;38:259–271.
27. Leitao A, Li M, Rodrigues AE. The role of intraparticle convection in protein adsorption by liquid chromatography using POROS 20 HQ/M particles. *Biochem Eng J*. 2002;11:33–48.
28. Chung SF and Wen CY. Longitudinal dispersion of liquid flowing through fixed and fluidized beds. *AIChE J*. 1968;14:857–866.
29. Books CA, Cramer SM. Steric mass-action ion exchange: displacement profiles and induced salt gradients. *AIChE J*. 1992;38:1969–1978.
30. Pedersen L, Mollerup J, Hansen E, Jungbauer A. Whey proteins as a model system for chromatographic separation of proteins. *J Chromatogr B*. 2003;790:161–173.
31. Whitley RD, Wachter R, Liu F, Wang NHL. Ion-exchange equilibria of lysozyme, myoglobin and bovine serum albumin-effective valence and exchanger capacity. *J Chromatogr*. 1989;465:137–156.
32. Graham LS, Broenda JH, Chase HA. Modeling single-component protein adsorption to the cation exchanger S Sepharose FF. *J Chromatogr*. 1990;498:113–128.
33. Hunter AK, Carta G. Effects of bovine serum albumin heterogeneity on frontal analysis with anion-exchange media. *J Chromatogr A*. 2001;937:13–19.
34. Houwing J, Jensen TB, van Hateren SH, van der Wielen LAM. Positioning of salt gradients in ion-exchange SMB. *AIChE J*. 2003; 49:665–674.
35. Houwing J, Billiet HAH, van der Wielen LAM. Optimization of azeotropic protein separations in gradient and isocratic ion-exchange simulated moving bed chromatography. *J Chromatogr A*. 2002;944: 189–201.

Appendix: Model Equations for Gradient TMB Model

In the gradient TMB model, the solid phase is assumed to move in plug flow in the opposite direction of the fluid phase, solid flow velocity as $u_S = L_C/t_{switch}$, while the inlet and outlet lines remain fixed. As a consequence, each column plays the same function, depending on its position (section).

Mass balance in a volume element of the bed in section j:

$$\frac{\partial C_{ij}}{\partial t} = D_{Lk}\frac{\partial^2 C_{ij}}{\partial Z^2} - \frac{u_j^{TMB}}{\varepsilon_B}\frac{\partial C_{ij}}{\partial Z} - \frac{(1-\varepsilon_B)}{\varepsilon_B}k_{Pij}\left[q_{ij}^* - q_{ij}\right] \quad \text{(A1)}$$

Mass balance in the particle

$$\frac{\partial q_{ij}}{\partial t} = u_S\frac{\partial q_{ij}}{\partial Z} + k_{Pij}(q_{ij}^* - q_{ij}) \quad \text{(A2)}$$

Initial conditions:

$$t = 0 : C_{ij} = q_{ij} = 0 \text{ for proteins} \quad \text{(A3a)}$$

before feed application to the column, a salt gradient has been formed in the columns as

$$C_{Sj} = C_S^D, \quad q_{Sj} = q_{Sj}^*(C_S^D) \text{ in sections I and II} \quad \text{(A3b)}$$

$$C_{Sj} = C_S^F, \quad q_{Sj} = q_{Sj}^*(C_S^F) \text{ in sections III and IV} \quad \text{(A3c)}$$

Boundary conditions in each section j for proteins and salt

$$D_{Lj}\varepsilon_B\left.\frac{\partial C_{ij}}{\partial Z}\right|_{Z=0} = u_j^{TMB}\left[C_{ij}\big|_{Z=0} - C_{ij,0}\right] \quad \text{(A4a)}$$

$$\left.\frac{\partial C_{ij}}{\partial Z}\right|_{Z=L_j} = 0 \quad \text{(A4b)}$$

$$\left.\frac{\partial q_{ij}}{\partial Z}\right|_{Z=0} = \left.\frac{\partial q_{ij-1}}{\partial Z}\right|_{Z=L_{j-1}} \quad \text{(A4c)}$$

$$q_{ij}\big|_{Z=0} = q_{ij-1}\big|_{Z=L_{j-1}} \quad \text{(A4d)}$$

Mass balances at nodes:

at the desorbent node,

$$C_{iI,0} = C_i^D \text{ open loop} \quad \text{(A5a)}$$

$$C_{iI,0} = \frac{Q_D C_i^D + Q_{IV}^{TMB} C_{iIV}\big|_{Z=L_{IV}}}{Q_I^{TMB}} \text{ closed loop} \quad \text{(A5b)}$$

at the extract node,

$$C_{iII,0} = C_{iI}\big|_{Z=L_I} \quad \text{(A5c)}$$

at the feed node,

$$C_{iIII,0} = \frac{Q_F C_i^F + Q_{II}^{TMB} C_{iII}\big|_{Z=L_{II}}}{Q_I^{TMB}} \quad \text{(A5d)}$$

at the raffinate node,

$$C_{iIV,0} = C_{iIII}\big|_{Z=L_{III}} \quad \text{(A5e)}$$

Global balances:

$$Q_I^{TMB} = Q_D - [\varepsilon_B/(1-\varepsilon_B)]Q_S \text{ open loop} \quad \text{(A6a)}$$

$$Q_I^{TMB} = Q_D + Q_{IV}^{TMB} \text{ closed loop} \quad \text{(A6b)}$$

$$Q_{II}^{TMB} = Q_I^{TMB} - Q_E \quad \text{(A6c)}$$

$$Q_{III}^{TMB} = Q_{II}^{TMB} + Q_F \quad \text{(A6d)}$$

$$Q_{IV}^{TMB} = Q_{III}^{TMB} - Q_R \quad \text{(A6e)}$$

The equivalence between gradient TMB model and gradient SMB model can be made in terms of flow rates, $Q_j^{TMB} = Q_j^{SMB} - [\varepsilon_B/(1-\varepsilon_B)]Q_S$, with $Q_S = (1-\varepsilon_B)V_c/t_{switch}$. Here L_C is column length, V_C is column volume, and t_{switch} is the switch time interval in gradient SMB operation.

Manuscript received Apr. 3, 2007, and revision received May 3, 2007.